

Polikristályos napelem modulok hőtechnikai modellje

A thermal model for polycrystalline solar modules

ifj.zsiboracs.henrik@gmail.com

¹University of Pannonia, Georgikon Faculty, PhD student

²University of Natural Resources and Life Sciences, Vienna, professor

³University of Natural Resources and Life Sciences, Vienna, PhD student

⁴University of Natural Resources and Life Sciences, Vienna, PhD student

⁵University of Natural Resources and Life Sciences, Vienna, technician

⁶Szent Istvan University, professor

⁷University of Pannonia, Georgikon Faculty, assistant professor

⁸University of Pannonia, Georgikon Faculty, associate professor

Nomenclature			
a_{pv}	PV absorptivity (-)	Q_{Rad}	long-wave radiation heat exchange (W)
A_{pv}	PV surface area (m ²)	Q_{Rem}	remaining heat on PV module (W)
I	incoming solar irradiance (W/m ²)	Q_{solar}	effective irradiation on PV module (W)
h_{force}	forced convection coefficient (W/(m ² K))	T_{PV}	PV module temperature (K or °C)
h_{free}	free convection coefficient (W/(m ² K))	T_{Amb}	Ambient temperature (K or °C)
h_{conv}	overall convection heat transfer (W/(m ² K))	v_{wind}	wind speed (m/s)
Q_{conv}	convective heat transfer on PV module (W)	ϵ_{pv}	PV emissivity (-)
Q_{PV}	PV output power (W)	σ	Stefan-Boltzmann's constant, 5,6697 x 10 ⁻⁸ (W/m ² K ⁴)

Introduction

Renewable energies have an increasing role in the process of energy production (Szabó et al., 2015, Horváth et al., 2015). Besides numerous other benefits, energy production based on solar performances can significantly contribute to sustainable energy management. By a one-time investment in solar PV technology, it is possible to produce CO₂-free, green energy for free without producing any waste for several decades (Hosenuzzaman et al., 2015, Aman et al., 2015, Zsiborács et al., 2016a).

The efficiency of solar energy utilization on Earth can be influenced by several factors. Silicon based crystalline solar modules are the most widespread worldwide. Under Hungarian climatic conditions, the temperature of crystalline solar modules can reach 60–70 °C on warm days. Due to its high temperature, the energy production of crystalline solar modules decreases. In the case of silicon based crystalline solar modules, efficiency decreases by 0.5% with 1 °C of temperature increase (Radziemska-Klugmann, 2002; Chandrasekar et al., 2015; Skoplaki et al., 2009, Zsiborács et al., 2016a, b, c, d, e).

We examined in this study a polycrystalline (p-Si) solar module (SL50TU-18P, 50W) under real climatic conditions on July 19th (09:00 am – 17:40 pm), installed on dual axis solar tracking system in Hungary, Keszthely. We determined by the help of this module the components of heat transfer.

Heat balance of polycrystalline solar module

The components of heat transfer are conduction, convection, and radiation. Only long-wave radiative (Q_{Rad}) and convective (Q_{Conv}) heat exchanges are considered for crystalline PV modules. Energy exchange in the form of electricity output by the PV module (Q_{PV}) is also considered. The solar radiation (Q_{Solar}) is collected by PV front surface. The difference between these four components ($Q_{\text{Solar}} - Q_{\text{Rad}} - Q_{\text{Conv}} - Q_{\text{PV}}$) gives the remaining heat energy (Q_{Rem}) of PV module (Tsai, 2014; Tsai-Tsai, 2012; Xu et al., 2009; Zsiboracs et al., 2016e).

The output power (Q_{PV}) was a measured value in this work. The net solar irradiation on polycrystalline solar module is given by (Tsai, 2014; Tsai-Tsai, 2012; Xu et al., 2009):

$$Q_{\text{solar}} = a_{\text{pv}} I A_{\text{pv}}. \quad (1)$$

The long-wave radiation heat exchange in the equivalent background environment (sky, ground, and surroundings) is given by (Tsai, 2014):

$$Q_{\text{Rad}} = \sigma \varepsilon_{\text{pv}} (T_{\text{pv}}^4 - T_{\text{Amb}}^4) A_{\text{pv}}. \quad (2)$$

The forced convection from the front surface is considered and is given by (Tsai, 2014; Agrawal-Tiwari,(2011):

$$Q_{conv} = h_{force}(T_{PV} - T_{Amb})A_{PV}. \quad (3)$$

$$h_{force} = 5,6 + 3,9v_{wind}. \quad (4)$$

On typical days, the overall convective heat transfer is the sum of the forced convection from the front surface and the free convection from the rear surface (Jones-Underwood, 2000; Tsai-Tsai, 2012; Tsai, 2014):

$$Q_{conv} = h_{conv}(T_{PV} - T_{Amb})A_{PV} \quad (5)$$

$$h_{conv} = h_{force} + h_{free} \quad (6)$$

$$h_{free} = 1,31\sqrt[3]{T_{PV} - T_{Amb}}. \quad (7)$$

Measurement site

The polycrystalline solar module was facing South with a tilt angle of 35° (table 1).

Table 1. Parameters of the p-Si solar module examined

Characteristics	Polycrystalline solar module
Country of origin	Italy
Manufacturer/Distributer	Energiesolaire100
Model	SL50TU-18P
Nominal performance (Pm) (W)	50
Performance tolerance (%)	±3%
Nominal tension (Vmp) (V)	19.12
Nominal current (Imp) (A)	2.62
Idling tension (Voc) (V)	22.68

Idling current (Isc) (A)	2.80
Module size (mm): (width x height x depth)	545x668x28

(Source: Data sheet from the manufacturer)

For the measurements two PicoLog data acquisition systems were used, one with 12 and one with 16 input channels. These instruments allowed second-based, continuous data recording by a PC (Zsiborács et al., 2015).

Additionally, the following technical-environmental parameters were determined:

- A Voltcraft VC607 professional multimeter, which was checked by an LT1021 device (10,000V \pm 5mV), was used for the calibration of the voltage and the current.
- The global radiation was measured by a pyranometer (OMSZ-certified. Eppley Black and White Model 4-48).
- The wind speed was measured by a JL-FS2, 4-20 mA, 3-spoon aluminium device.
- For measuring the temperatures, Pt 100 sensor was used with the help of the PicoLog devices. The calibration of the whole temperature measurement system was done using an LM 35 digital thermometer with a lineal voltage change (+ 10.0 mV/°C, 0.1 V = 1 °C, 1 V = 100 °C) and an accuracy of \pm 1/4 °C at room temperature and that of \pm 3/4 °C between -55 and $+ 150$ °C (Zsiborács et al., 2015; Zsiborács et al., 2016a, b, c, d).
- A True Maximum Point Seeking (TMPS) device, which maintained the maximum power point (MPP) was used for the measurements (Figs. 1 and 2).

The schematic diagram of the measurement point is shown in Figure 3.

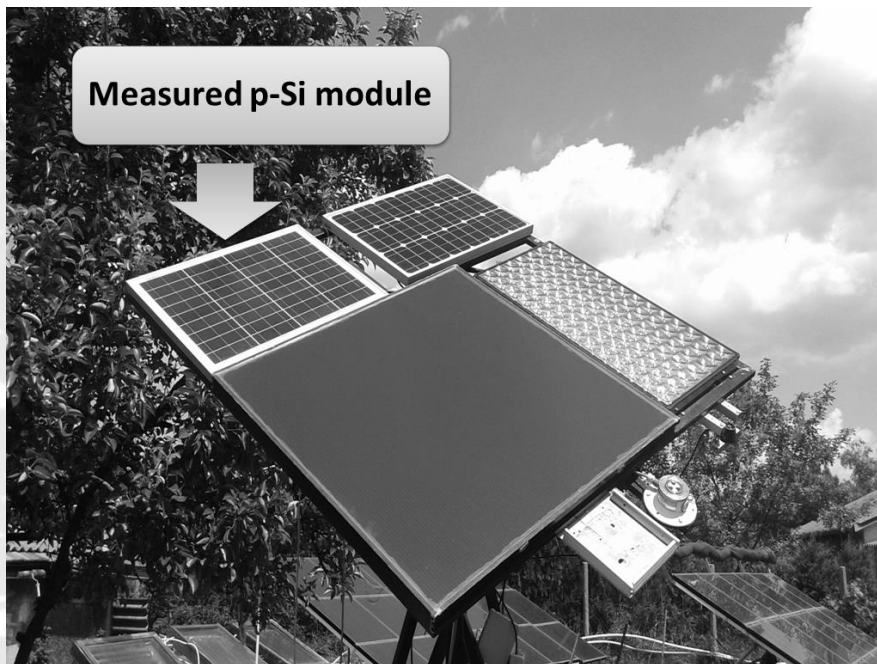


Figure 1. The measuring station of the photovoltaic system in Keszthely



Figure 2. The wind speed sensor anemometer. (Zsiborács et al., 2016a)

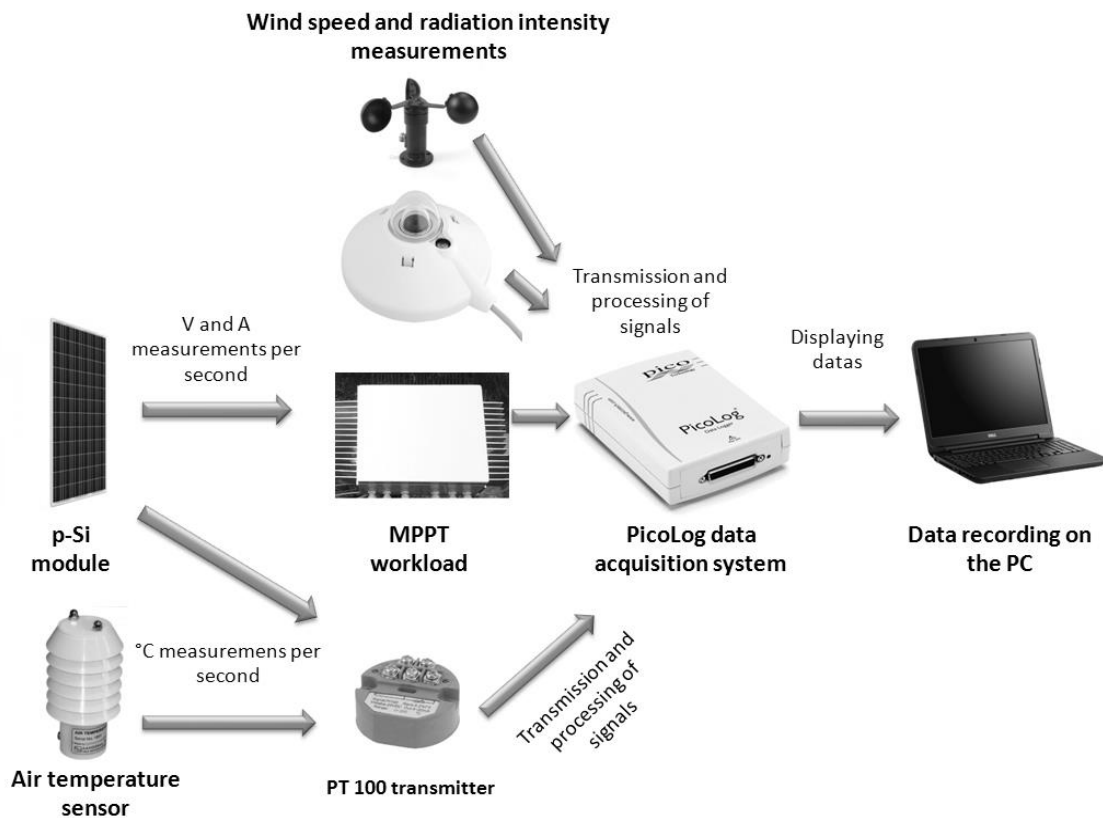


Figure 3. Schematic illustration of solar module measuring station

Results of the thermal measurement of the polycrystalline solar module

We carried out the thermal analysis of the p-Si module from 09:00 to 17:40 on 19th July, since at that time the environmental and experimental conditions were the most favourable for the test. In calculating the results the time factor was also taken into account. So we have interpreted the values as energy (Wh). The values of the thermal energy of p-Si solar module is related to the differences in the areas of the modules, their specific heat and mass. During the nearly 9 hour measurement period, the great majority of the solar radiation appeared as remaining heat energy (Q_{Rem}) in the structure of the p-Si solar modules 38%, thus increasing the temperature of the modules. According to our measurements the percentage of daily energies were the following: Q_{Rem} : 38%, Q_{Rad} : 19%, Q_{Conv} : 29% and Q_{PV} : 14%. Clearly visible that the Q_{Rem} was the highest value which caused the high PV module temperature (Figure 4).

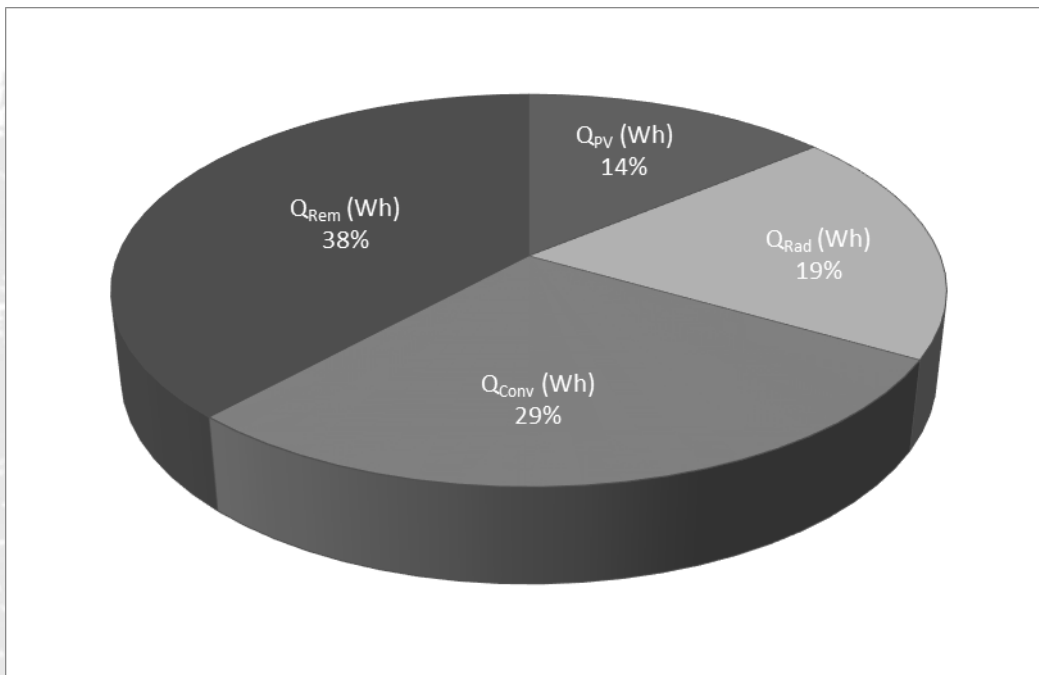


Figure 4 Daily energy distribution at the p-Si module (July 19th from 09:00 am to 17:40 pm)

Conclusion

We examined in this study a polycrystalline solar module (SL50TU-18P, 50W) under real climatic conditions on July 19th (09:00 am – 17:40 pm), installed on dual axis solar tracking system in Hungary, Keszthely. We determined by the help of this module the components of heat transfer. During the nearly 9 hour measurement period, the great majority of the solar radiation appeared as remaining heat energy (Q_{Rem}) in the structure of the p-Si solar modules 38%, thus increasing the temperature of the modules. Due to its high temperature, the energy production of solar modules decreases, however, this could be solved by various cooling technologies like air based, water based, heat exchanger / coolant based and heat based categories.

Acknowledgements

We acknowledge the financial support of Széchenyi 2020 under the **EFOP-3.6.1-16-2016-00015**.

References

1. Agrawal, S. – Tiwari, G.N. (2011): Performance evaluation of hybrid modified micro-channel solar cell thermal tile: an experimental validation. *International Journal of Engineering, Science and Technology*, 3(1) 244-254. p.
2. Aman, M.M. – Solangi, K.H. – Hossain, M.S – Badarudin, A. – Jasmon, G.B. – Mokhlis, H. – Bakar, A.H.A. – Kazi S.N. (2015): A review of Safety, Health and Environmental (SHE) issues of solar energy system. *Renewable and Sustainable Energy Reviews*, 1190-1204. p.
3. Chandrasekar, M., Rajkumar, S., Valavan, D. (2015). A review on the thermal regulation techniques for non integrated flat PV modules mounted on building top. *Energy and Buildings*, 86, 692-697.
4. Hosenuzzaman, M. – Rahim, N.A. – Selvaraj, J. – Hasanuzzaman, M. – Malek, A.B.M.A. – Nahar, A. (2015): Global prospects. progress. policies. and environmental impact of solar photovoltaic power generation. *Renewable and Sustainable Energy Reviews*, 41, 284-297. p.
5. Horváth M., Kassai-Szoó D., Csoknyai T., 2016: Solar energy potential of roofs on urban level based on building typology. *Energy Buildings* 111, 278–289.
6. Radziemska, E. – Klugmann, E. (2002): Thermally affected parameters of the current–voltage characteristics of silicon photocell. *Energy Conversion and Management*, 43(14), 1889-1900. p.
7. Skoplaki, E. – Palyvos, J.A. (2009): Operating temperature of photovoltaic modules: A survey of pertinent correlations. *Renewable Energy*, 34(1), 23-29. p.
8. Szabó Sz., Enyedi P., Horváth M., Kovács Z., Burai P., Csoknyai T., Szabó G., 2015: Automated registration of potential locations for solar energy production with Light Detection And Ranging (LiDAR) and small format photogrammetry. *J. Cleaner Product* 112, 3820–3829.
9. Tsai, H-L. (2014): Design and Evaluation of a Photovoltaic/Thermal-Assisted Heat Pump Water Heating System. *Energies*, 7, 3319-3338. p.
10. Tsai, H-F. – Tsai, H-L. (2012): Implementation and verification of integrated thermal and electrical models for commercial PV modules. *Solar Energy*, 86, 654-665. p.
11. Xu, G. – Deng, S. – Zhang, X. – Yang, L. – Zhang, Y. (2009): Simulation of a photovoltaic/thermal heat pump system having a modified collector/evaporator. *Solar Energy*, 83, 1967-1976. p.
12. Zsiborács, H. – Pályi, B. – Baranyai, H.N. –Veszélka, M. – Farkas, I. – Pintér, G. (2016a). Energy performance of the cooled amorphous silicon photovoltaic (PV) technology. *Időjárás*,121(1)415-430 .p.
13. Zsiborács, H. – Pályi, B. – Baranyai, N.H. – Pinter, G. – Farkas, I. (2016b): Hűtött amorfszilícium napelem teljesítmény többleszámának vizsgálata. LVIII. Georgikon Napok, 463-471. p.
14. Zsiborács, H. – Pályi, B. – Pintér, G. (2015): Permetezett monokristályos napelemek vizsgálata. LVII. Georgikon Napok, 505-514. p.
15. Zsiborács, H. – Pályi, B. – Pinter, G. – Baranyai, N.H. – Szabó P. – Farkas, I. (2016c): Economic aspects and energy performance of the cooled polycrystalline solar photovoltaic (PV) technology. *Review on Agriculture and Rural Development*, 5(1-2), 162-170. p.
16. Zsiborács, H. – Pályi, B. – Pintér, G. – Popp, J. – Balogh, P. – Gabnai, Z. – Pető, K. – Farkas, I. – Baranyai, N.H. – Bai, A. (2016d): Technical-economic study of cooled crystalline solar modules. *Solar Energy*, 140, 227-235. p.
17. Zsiborács, H. – Weihs, P. – Trimmel, H. – Oswald, S. – Pályi, B. (2016e): A thermal model for monocrystalline solar modules. 22nd Workshop on Energy and Environment. 15. p.